Sustainable Food Technology

ROYAL SOCIETY OF CHEMISTRY

PAPER

View Article Online
View Journal

Cite this: DOI: 10.1039/d5fb00806a

Effect of cold plasma pre-treatment on drying kinetics and nutritional compounds of sweet lime peel

Gurveer Kaur, Sandhya Singh,* Vimal Challana * and Sumandeep Kaur

Sweet lime fruits are cherished for their characteristic aroma, refreshing taste, and abundance of bioactive compounds. Cold plasma (CP) is an emerging non-thermal technology that offers a promising approach to enhance drying efficiency while preserving the nutritional and functional quality of food products. The study evaluated the effect of CP pre-treatment at different exposure times (5, 10 and 15 minutes) on the hot-air drying behavior and quality attributes of sweet lime peel (SLP). The CP pre-treatment significantly accelerated the drying rate, reducing the drying time by about 45 minutes. By accelerating drying while minimizing energy use and nutrient loss, the process advances sustainable food processing by improving efficiency and reducing environmental impact. Among the drying models tested, the logarithmic model best fit the experimental data, with high accuracy (R^2 > 0.990, χ^2 < 0.009, RMSE < 0.033). However, the artificial neural network (ANN) model outperformed the traditional approach, achieving superior predictive performance for the moisture ratio. The optimal network configuration was a three-layered topology with 17 hidden-layer neurons, yielding the lowest MSE, RMSE, and χ^2 values. Microstructural analysis revealed that CP exposure led to surface etching and the formation of microchannels by reactive plasma species, thereby enhancing moisture diffusion and improving bioactive retention. CP-treated samples showed marked improvement in rehydration ratio (2.96–3.37), total phenolic content (18.74–26.53 mg GAE per g), total flavonoid content (15.23–26.73 mg QE per g), antioxidant activity (32.38–44.88%), and ascorbic acid content (60.12–82.28 mg/100 g). These results indicate that CP pretreatment is an effective and sustainable technique for improving the drying performance and nutritional quality of fruit by-products.

Received 31st October 2025
Accepted 26th March 2026

DOI: 10.1039/d5fb00806a

rsc.li/susfoodtech

Sustainability spotlight

This study promotes sustainable food processing by utilizing cold plasma pretreatment to enhance the drying efficiency and nutritional retention of sweet lime peel, a major citrus by-product. The process significantly reduced drying time by nearly 45 minutes while improving bioactive compounds such as phenolics, flavonoids, and antioxidants, thereby transforming a commonly discarded material into a value-added ingredient. By accelerating drying and reducing energy consumption without compromising product quality, the technique advances eco-efficient and waste-minimizing food manufacturing. Through these outcomes, the research contributes to SDG 2 (Zero Hunger) by promoting the utilization of nutrient-rich by-products in the food chain, SDG 9 (Industry, Innovation, and Infrastructure) by encouraging the adoption of innovative non-thermal and energy-efficient drying technologies, and SDG 12 (Responsible Consumption and Production) by supporting circular economy principles and reducing post-harvest and processing waste.

1 Introduction

Citrus fruits are among the most extensively cultivated crops globally, with China, Brazil, and India leading production.[1] Around one-third of the total citrus yield, over 88 million tons annually, is processed into juice, marmalade, and essential oils. However, processing generates more than 15 million tons of waste per year, mainly comprising peel, pulp, and seeds.[2] These residues are rich in proteins, phenolics, vitamins, lipids, minerals, and fibres, but are often discarded, causing environmental and economic concerns. Among citrus varieties, *Citrus limetta,* commonly known as sweet lime or mosambi, is particularly notable for its nutritional composition and therapeutic properties. It contains essential micronutrients and a diverse range of bioactive compounds, including flavonoids, limonoids, volatile oils, coumarins, alkaloids, sterols, and carotenoids. These phytochemicals exhibit potent antioxidant, antimicrobial, and anticancer properties. Despite this biochemical richness, sweet lime residues, especially peels and seeds, are underutilized and often discarded, contributing to

Department of Processing and Food Engineering, College of Agricultural Engineering and Technology, Punjab Agricultural University, Ludhiana-141004, Punjab, India. E-mail: vimalchallana@gmail.com; sandhya-pfe@pau.edu

waste management challenges. The valorization of such by-products offers an opportunity to recover natural antioxidants, dietary fibers, and other functional ingredients, supporting the principles of circular economy and sustainable utilization of agricultural waste.[3] However, the effective utilization of sweet lime peel is constrained by its high initial moisture content and slow drying behavior, which limit its industrial applicability.

Drying plays a crucial role in the processing and preservation of fruit by-products, particularly for the recovery of bioactive compounds from peels. It reduces moisture to safe levels, thereby extending shelf life and enabling further processing such as grinding and extraction.[4] However, conventional drying is often slow and may adversely affect the stability of heat-sensitive components. To mitigate these limitations, pre-treatments such as blanching, alkaline dipping, and sulphating have been employed to enhance drying efficiency and product quality.[5] Nevertheless, these methods may induce nutrient loss, undesirable sensory changes, and potential health or environmental concerns.

In recent years, non-thermal pre-treatment technologies have gained attention as sustainable alternatives. Treatments such as ultrasonication, microwave heating, and pulsed electric fields have improved drying performance while minimizing quality degradation. Among these, cold plasma (CP) has emerged as a particularly attractive eco-friendly approach due to its potential to inactivate enzymes, induce surface microstructural modification, and enhance moisture diffusion without significant thermal damage.[6] The reactive species generated during CP treatment induce controlled surface modifications which enhance moisture diffusion and drying rate while preserving thermolabile components.

Drying is a complex and non-linear process influenced by multiple interacting variables. Conventional drying models often produce higher prediction errors under modified processing conditions. Artificial neural network modeling can capture these complex relationships and predict drying behavior with lower error using similar input parameters.

Despite growing interest in CP-assisted drying, limited information is available regarding its application to sweet lime peel. Therefore, the present study investigates CP as an eco-friendly pretreatment before hot-air drying of *Citrus limetta* peel. The study examines changes in drying kinetics and moisture diffusion behavior, evaluates the retention of nutritional and functional quality, and analyzes the influence of plasma pretreatment on bioactive compound extraction. Thin-layer drying models and artificial neural network approaches are employed for predictive modeling. The findings aim to support sustainable utilization of sweet lime peel through improved processing strategies.

2 Materials and methods

2.1. Raw material

The sweet lime peels (SLP) were sourced from a local fruit juice vendor in Ludhiana. The peels were sorted based on thickness and appearance. The peels were cut into even rectangular slices. The peels were stored at 4 °C until further use.

2.2. Moisture

The moisture content of the peels was determined according to the procedure described by Shirkole *et al.* (2025).[7] Peels of 5–6 g were dried in a Petri dish in a hot-air oven at 105 °C until successive weight measurements showed no significant change.

2.3. Cold plasma pre-treatment

The laboratory-scale dielectric barrier discharge (DBD) system generates CP. The chamber used for plasma generation was constructed from 8 mm thick glass with internal dimensions of 50 cm × 30 cm × 30 cm. The dielectric barrier consists of copper foils as electrodes and Pyrex glass, which works as dielectric layers. The system is equipped with an extra-high-tension transformer (used for a high-voltage power supply) capable of generating voltages in the 32- and 47 kV ranges. A switch-mode supply was used to convert the AC input (220 V) to a DC output of 12–14 V. A frequency of 25 kHz was maintained *via* a frequency setup integrated into the setup. The setup also includes an LCD for real-time discharge-voltage monitoring and a voltage controller to adjust the discharge output voltage as needed. All the components were integrated into a Pyrex glass chamber to ensure safety and efficient plasma generation.

The selection of applied voltage and exposure time was based on preliminary trials conducted. During these trials, the SLPs were treated at different voltage levels (35, 40, and 45 kV) with exposure times ranging from 5 to 15 min to assess the effect on drying behavior. The observations demonstrated that increasing the applied voltage improved treatment effectiveness, reducing the time required to reach the target moisture content. Treatment performed at 35 kV resulted in only marginal reductions in drying times (nearly 140–145 min), while moderate improvement was observed at 40 kV (approximately 125–145 min). In contrast, treatment at 45 kV resulted in a substantial reduction in drying time (approximately 96–129 min) compared with the untreated or controlled sample. Based on these observations, 45 kV was selected as the operating voltage for the present study and treatment durations of 5, 10, and 15 min were chosen to evaluate the effect of exposure time. The inter-electrode spacing was maintained at 3 cm, and approximately 10–12 g of SLP was used for each treatment.

2.4. Hot-air drying experiment

SPL samples were dried under hot air using a lab-scale convective dryer (440 V, Kilburn Laboratory, India) with 1370 × 940 × 430 mm (Fig. 1). The dryer consists of a drying chamber, trays, a blower/fan, a heating coil, a temperature control system, air inlet and exhaust vents, a digital display panel, and a frame and insulation.[8] SPL was dried at 70 °C with a constant airflow rate of 1 m s^{-1}. Periodic weight measurements were recorded every 15 minutes using a digital weighing scale throughout the drying process. The process was continued until SLP reached a final moisture content of less than 10%.

2.5. Drying kinetics

The weight recorded for all the samples was used to calculate moisture loss using the following eqn (i).[8] The drying rate (DR)

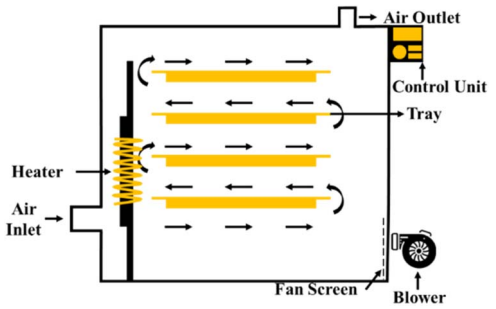

Fig. 1 Hot air dryer.

and moisture ratio (MR) of SLP were calculated using equations (ii)[9] and (iii),[10] respectively.

$$M_t = \frac{m_k - m_p}{m_p} \quad \text{(i)}$$

$$MR = \frac{M_t}{M_0} \quad \text{(ii)}$$

$$DR = \frac{M_{t+dt} - M_t}{dt} \quad \text{(iii)}$$

where, M_t is the moisture content of SLP (dry basis) at time t, m_k is the mass at any time t, m_p is mass of absolutely dried SLP (g), M_0 is the moisture content of SLP (dry basis) at $t = 0$, M_{t+dt} is the moisture content at time $t + dt$, dt is the increment in the time of drying (min).

The drying process involves several transport phenomena, such as surface diffusion, molecular diffusion, Knudsen diffusion, capillary flow, evaporation, and condensation. These mechanisms collectively estimate the moisture migration from the internal structure to the surface of food products. The mass transfer rate due to molecular diffusion is directly linked to the moisture gradient and can be quantified using the effective moisture diffusivity (D_{eff}) coefficient.[11] D_{eff} can be calculated using the following equation:

$$\ln(MR) = \ln\left(\frac{8}{\pi^2}\right) - \left(\frac{\pi^2 \cdot D_{eff} \cdot t}{4 \cdot L^2}\right) \quad \text{(iv)}$$

where, MR is the fractional moisture ratio, D_{eff} is effective moisture diffusivity, t denotes the drying time (s), and L is the half thickness of the sample (m).

The experimental MR data as a function of drying time were fitted using mathematical models commonly used to determine the most appropriate models for predicting SLP drying kinetics (Table 1). Coefficient of determination (R^2), root mean square error (RMSE), and chi-square (χ^2) were used to evaluate the performance of the model and select the best model that assesses the goodness of fit.

2.6. Artificial neural network

MATLAB software (R2018a, MathWorks, USA) was employed to develop and assess Artificial Neural Network (ANN) models. The input, hidden, and output layers are the three main layers on the surface of an ANN, constructed using a feed-forward topology (Fig. 2). The network designed in this study has two neurons in the input layer and several neurons in the hidden layer. A trial-and-error approach was adopted to identify the optimal number of hidden neurons (1–20). An excessive number of neurons can lead to overfitting and prolong training time, whereas a limited number can lead to underfitting. The dataset was randomly divided into training (70%), validation (15%), and testing (15%) subsets to ensure reliable model evaluation. The predictive performance of the ANN model was compared with that of conventional mathematical drying models to assess model fit and predictive capability.

Table 1 The mathematical models used for drying curves

Model	Equation	Reference
Lewis	$MR = \exp(-kt)$	12
Henderson and Pabis	$MR = a\exp(-kt)$	13
Page	$MR = \exp(-kt^n)$	14
Modified Page	$MR = \exp(-(kt)^n)$	15
Logarithmic	$MR = a\exp(-kt)+b$	16
Wang and Singh	$MR = 1 + at + bt^2$	17

MR—product water content ratio (dimensionless); k—drying constants (1/min); a, b, c, n—constants of the models (dimensionless); t—drying time (min); n—equation number.

2.7. Microstructure analysis

Sections of the peel extending from the epidermis to the peel–pulp interface were carefully collected. The samples were then subjected to critical-point drying and coated with a thin gold layer using a sputter coater (108 Auto, Cressington Scientific Instruments, Watford, UK) to ensure adequate electrical conductivity prior to analysis. The prepared samples were examined using a scanning electron microscope (SEM; JSM-IT800, JEOL Ltd., Akishima, Tokyo, Japan).

2.8. Rehydration ratio

The rehydration ratio (RR) was used to evaluate the ability of dried SLP to absorb and regain its original structure and texture. The RR was estimated per the method described by Bai *et al.* (2025).[18] Approximately 5 g of dried SLP was immersed in distilled water at 95 °C for 60 min. After excess moisture was

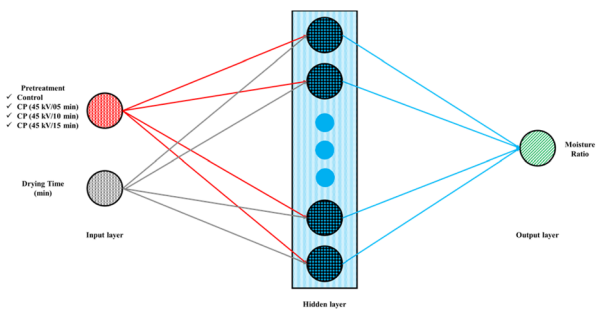

Fig. 2 ANN model configuration.

removed using filter paper, and samples were reweighed. RR can be calculated using the following equation:

$$RR = \frac{W_f}{W_i} \quad (v)$$

where W_i is the weight of the dried sample, and W_f is the weight of the rehydrated sample.

2.9. Phytochemical properties of sweet lime peel powder

The dried SLP was ground using a multifunctional food processor (Bajaj Electricals Limited, Model: FX11 600 Watts Food Processor).

2.9.1. Extraction. The sample extract was prepared per the procedure described by Zhou *et al.* (2020)[19] with slight modifications. In brief, 1 g of dried sample was extracted with 25 mL of ethanol solution (80%, v/v) in an ultrasonic bath at room temperature (40 °C) for 30 min. The mix was then centrifuged at 8000×*g* for 10 min at 4 °C. The extraction procedure was repeated twice for residue extraction, and the combined supernatants from both extractions were used for further analyses.

2.9.2. Total phenolic content and total flavonoid content. Total phenolic content (TPC) and total flavonoid content (TFC) were determined according to the Folin–Ciocalteu colorimetric and aluminum chloride colorimetric assays, respectively, following the methodology described by Phuyal *et al.* (2020).[20] Absorbance was recorded at 760 nm (TPC) and 510 nm (TFC) with the help of a UV-Vis spectrophotometer (UV–2601; Rayleigh, Beijing Shi, China), with results expressed as gallic acid equivalents (GAE)/g dry weight and mg quercetin equivalents (QE)/g dry weight.

2.9.3. DPPH radical scavenging activity. The radical scavenging activity of the SLP powder extract was calculated using the 1,1-diphenyl-2-picryl hydrazyl (DPPH) technique as per the methodology described by Baliyan *et al.* (2022).[21] Absorbance of the sample was determined at 517 nm. The percentage of antioxidant radical scavenging activity can be calculated by using the following equation:

$$\%\ DPPH = \frac{\text{Absorbance}_{\text{Control}} - \text{Absorbance}_{\text{Sample}}}{\text{Absorbance}_{\text{Control}}} \times 100 \quad (vi)$$

2.9.4. Ascorbic acid. The ascorbic acid content in SLP powder was estimated by the 2,6-dichloroindophenol titrimetric method.[22]

2.10. Statistical analysis

The experiment was conducted in triplicate, and data are reported as mean ± standard deviation. Statistical analyses were performed using Minitab version 18.1 (Minitab Inc., USA). Before analysis, the assumptions of normality and homogeneity of variance were evaluated using the Shapiro–Wilk and Levene's tests, respectively, and the results confirmed that the data satisfied both assumptions required for Analysis of Variance ($p > 0.05$). The experimental analysis used a one-way ANOVA with the Tukey post hoc test ($p < 0.05$) to assess significant differences among groups.

3 Results and discussion

3.1. Drying kinetics

The drying behavior of SLP under different CP pretreatments was depicted in Fig. 3. In all samples, MR decreased continuously with increasing drying time. However, a faster drying rate was observed in the samples pre-treated with CP, indicating enhanced drying efficiency. Among all the pre-treatments, CP at 45 kV for 15 minutes showed the fastest drying, followed by 10 and 5 minutes treatments, while the control sample took the longest drying time. This clearly indicates that the CP pretreatment facilitates the moisture diffusion during drying.

The improvement in drying rate results from CP's effects on the SLP surface, as shown in Fig. 4. CP generates high-energy ions, and reactive species collide with the SLP surface, causing physical and chemical modifications, including surface etching, microcrack formation, and cell wall disruption. These changes increase the surface porosity, facilitating the moisture diffusion and accelerating the drying rate as treatment time increases.[23] Nevertheless, the enhanced drying rate cannot be attributed solely to plasma-induced microchannels; both surface-level modifications and possible alterations in the internal cellular structure may also contribute to improved moisture transport. Reactive oxygen species (ROS) generated during CP treatment interact with the peel surface, forming oxygen-containing functional groups, such as hydroxyl and carboxyl. These groups enhance the surface affinity towards the water molecules, facilitating easier adsorption and subsequent diffusion of moisture.[18,24,25] These surface chemical modifications may mainly affect the initial removal of moisture from the material surface, whereas structural disruptions within the tissue may influence the migration of moisture from the interior.

The effective moisture diffusivity values were tabulated in Table 2, ranging from 4.493×10^{-7} m^2 s^{-1} (control) to 6.874×10^{-7} m^2 s^{-1} (CP/15 min). The diffusivity increased with prolonged CP exposure, indicating enhanced internal moisture migration. This increase may be attributed to changes in internal mass transfer pathways resulting from plasma-induced structural modifications in the peel matrix. The diffusivity recorded for CP/15 min was approximately 53% higher than that of the control sample, reflecting the impact of CP on moisture migration.

Similarly, increased CP exposure reduced the drying time required to reach a 10% final moisture content. The increase in treatment duration may promote greater structural disruption and surface etching, which together facilitate moisture removal. The control sample required nearly 149.5 min, while CP pretreated samples showed progressive reduction, with the shortest time of nearly 96 min for CP/15 min (as show in Table 2). This represents a 36% reduction in drying time compared to the control. These findings were consistent with earlier findings by Zhang *et al.* (2019)[26] who observed improved drying rates in CP-treated chili peppers. Similarly, Bai *et al.* (2025)[18] reported a nearly 18% reduction in drying time for peas exposed for 90 and 120 seconds. The results clearly showed that plasma

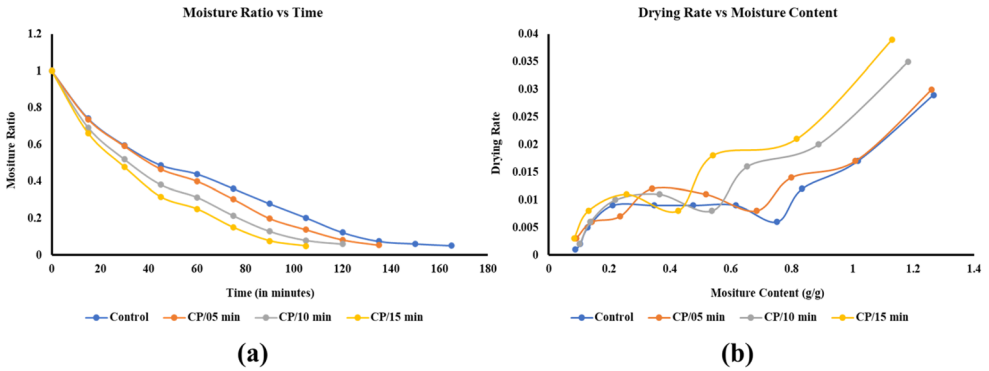

Fig. 3 (a) Moisture ratio and (b) drying rate of sweet lime peels under different cold plasma treatments.

pretreatment increases the effective moisture diffusivity, suggesting modifications in both surface properties and internal moisture–transport pathways within the sweet lime peel matrix.

3.2. Mathematical modeling

The obtained drying data were analyzed to describe the hot-air drying kinetics of SLP pre-treated with CP. The experimental moisture ratio values were fitted using non-linear regression analysis with commonly applied models: Lewis, Page, Modified Page, Henderson & Pabis, Wang & Singh, and Logarithmic. The statistical parameters, including R^2, RMSE, and χ^2, obtained from all the models are presented in Table 3.

All models show a strong fit to the experimental data, as evidenced by high R^2 values exceeding 0.97. Other analyzed parameters, such as RMSE, ranged from 0.0086 to 0.0475, and χ^2 values varied from 0.0021 to 0.0226 across models. Comparing the statistical data from the models, the Logarithmic model provided the best overall fit for both treated and untreated samples. The model achieved an R^2 value above 0.990, a χ^2 value of 0.0021, and an RMSE below 0.033. The findings are consistent with several studies, which have shown that the Logarithmic model best describes the drying behavior of diverse agricultural commodities. Kalsi *et al.* (2023)[8] showed that the logarithmic model provided the best fit to the experimental data, with R^2 values > 0.9952 and the lowest RMSE and χ^2 values. Similarly,

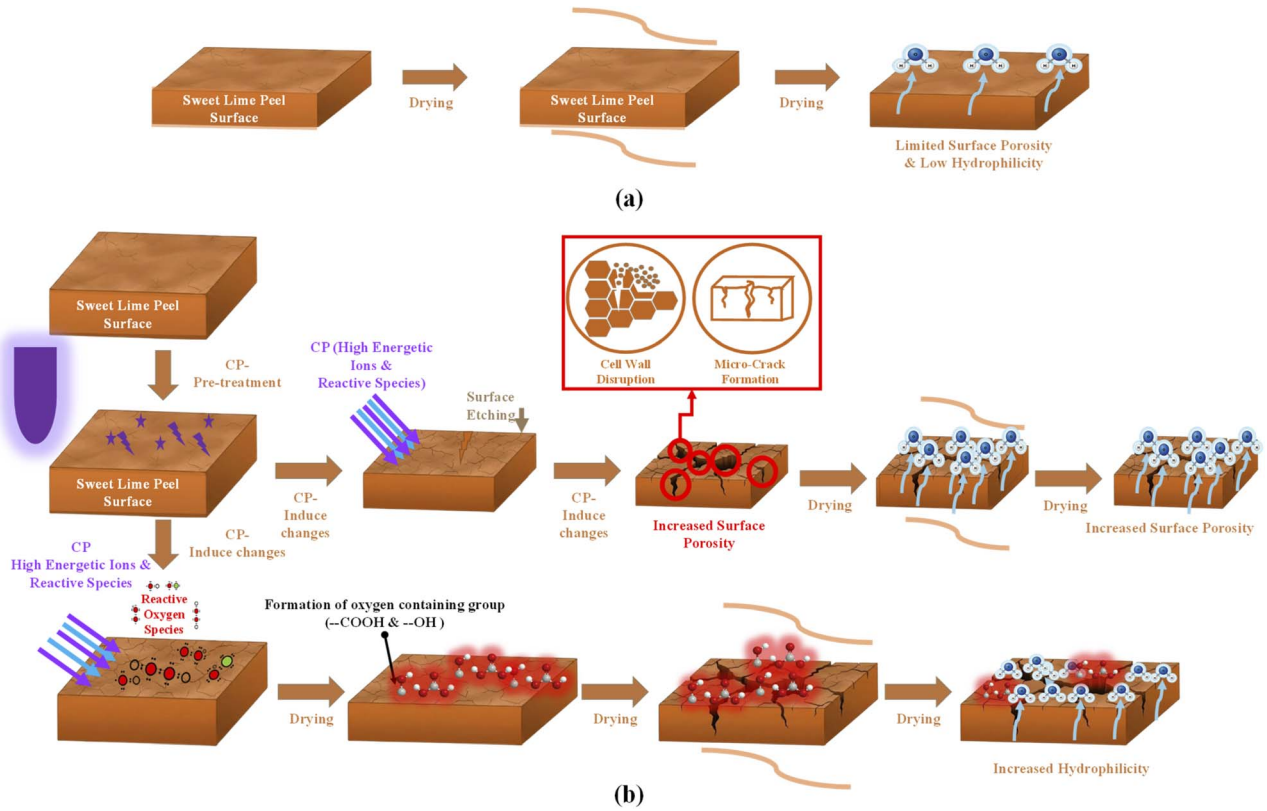

Fig. 4 Control drying (a) and cold plasma pre-treatment–induced accelerated drying mechanism (b).

Table 2 Moisture diffusivity and drying time of SLP under different treatments

Sample	Slope (m)	Thickness (mm)	Moisture diffusivity (x 10^{-7} m^2 s^{-1})	Time to 10% moisture (min)
Control	−0.2769	4	4.493	149.523
CP/05 min	−0.3132	4	5.083	129.315
CP/10 min	−0.3516	4	5.706	112.133
CP/15 min	−0.4236	4	6.874	95.97

Chen *et al.* (2015)[27] highlighted the Logarithmic model as effective for predicting hot-air drying of jujube slices, with lower RMSE values. Akpinar and Bicer (2008)[28] also observed that thin-layer drying of long green peppers under solar and open-sun conditions was best represented by the Logarithmic model, with $R^2 = 0.9882$, $\chi^2 = 0.00174$, and RMSE = 0.0410.

3.3. ANN modelling

An ANN model was developed in this study to predict the MR of hot-air-dried SLP as a function of pre-treatment and drying time. A multi-layer feed-forward topology was used to develop the ANN model. The topology was evaluated to identify the optimal number of hidden neurons with the least MSE, RMSE, and χ^2. Fig. 5 provides the relationship between the artificial neural network performance and the number of neurons in the hidden layer. Among all the models, the optimal network configuration was a three-layer network with 17 hidden neurons. The 17 hidden neurons had the least value for MSE, RMSE, and χ^2.

Fig. 6a illustrates the training performance of the ANN model in terms of MSE for the training, validation and testing datasets. The model achieved its validation performance early in training, indicating rapid convergence and effective generalization while preventing overfitting.

Fig. 6(b) illustrates the training state of the ANN model in terms of gradient magnitude, Levenberg–Marquardt parameter (μ), and validation checks as a function of training epochs. The gradual decline in gradient and μ values indicates stable convergence and

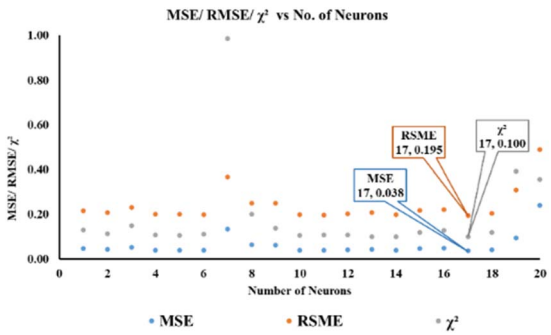

Fig. 5 Evaluation of ANN performance based on the number of neurons in the hidden layer for hot-air drying of SLP.

Table 3 Mathematical models for predicting moisture ratio and regression analysis with statistical parameters in hot-air drying of sweet lime peel

Model	Treatment	Estimated coefficients	R^2	χ^2	RMSE
Lewis	Control	$k = 0.01567$	0.98536	0.01445	0.01445
	CP/05 min	$k = 0.01748$	0.98990	0.00862	0.00862
	CP/10 min	$k = 0.02159$	0.99518	0.0038	0.0038
	CP/15 min	$k = 0.02544$	0.99647	0.00264	0.00264
Page	Control	$k = 0.01637$, $n = 0.98985$	0.98392	0.0144	0.038
	CP/05 min	$k = 0.01530$, $n = 1.03177$	0.98903	0.00832	0.0322
	CP/10 min	$k = 0.02361$, $n = 0.97756$	0.99464	0.0037	0.0279
	CP/15 min	$k = 0.02577$, $n = 0.99673$	0.99588	0.00265	0.0272
Modified Page	Control	$k = 0.01569$, $n = 0.99099$	0.98392	0.01442	0.03795
	CP/05 min	$k = 0.01740$, $n = 1.03543$	0.98903	0.00832	0.03232
	CP/10 min	$k = 0.02167$, $n = 0.97860$	0.99464	0.0037	0.02294
	CP/15 min	$k = 0.02546$, $n = 0.99707$	0.99588	0.00264	0.02155
Henderson & Pabis	Control	$a = 0.98217$, $k = 0.01538$	0.98588	0.01393	0.0373
	CP/05 min	$a = 0.9958$, $k = 0.0174$	0.98993	0.00859	0.0327
	CP/10 min	$a = 0.98977$, $k = 0.02136$	0.99536	0.00366	0.0229
	CP/15 min	$a = 0.99538$, $k = 0.02533$	0.9965	0.00262	0.0209
Wang & Singh	Control	$a = -0.01187$, $b = 3.77483 \times 10^{-5}$	0.9771	0.02259	0.0475
	CP/05 min	$a = -0.01344$, $b = 4.8723 \times 10^{-5}$	0.98653	0.0115	0.0379
	CP/10 min	$a = -0.01663$, $b = 7.51231 \times 10^{-5}$	0.98406	0.01258	0.0424
	CP/15 min	$a = -0.01934$, $b = 1.00582 \times 10^{-4}$	0.98567	0.01072	0.0423
Logarithmic	Control	$a = 1.059$, $b = -0.0999$, $k = 0.01224$	0.99004	0.00983	0.033
	CP/05 min	$a = 1.098$, $b = -0.1249$, $k = 0.01339$	0.99472	0.00451	0.0254
	CP/10 min	$a = 1.017$, $b = -0.0345$, $k = 0.01964$	0.99603	0.00314	0.0229
	CP/15 min	$a = 1.022$, $b = -0.0337$, $k = 0.02332$	0.9972	0.0021	0.0205

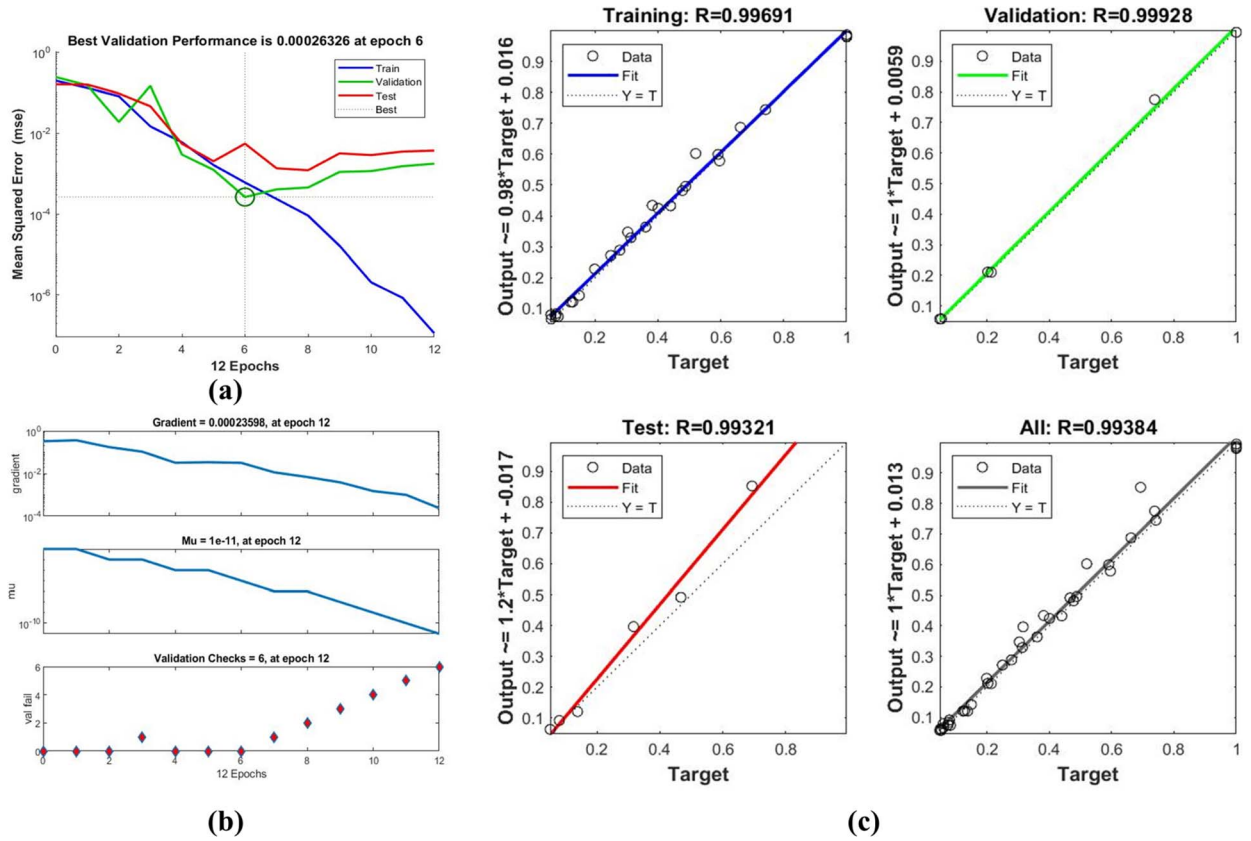

Fig. 6 Training and performance evaluation of the ANN model for MR of hot-air dried SLP (a); with corresponding performance plots (b); and comparison between experimental and predicted (c).

effective weight optimization. The increase in validation checks at the final epoch confirms the activation of early stopping, preventing overfitting and ensuring good generalization.

Fig. 6(c) presents the regression analysis of experimental and ANN-predicted moisture ratios for the training, validation, testing, and overall datasets. The predicted values closely follow the 1 : 1 line, with high correlation coefficients across training ($R = 0.99691$), validation ($R = 0.99928$), testing ($R = 0.99321$), and the overall dataset ($R = 0.99384$), confirming the ANN model's high predictive accuracy and reliability.

Previous studies have used similar approaches to predict MR using ANN modelling. Khaled *et al.* (2020)[29] reported that the optimal ANN for predicting MR in hot-air-dried persimmon fruit has 2 hidden layers with 6 neurons. Similarly, Kalsi *et al.* (2023)[8] found that a three-layered topology with 16 neurons best modelled convective hot air-dried stevia leaves, while in another study, Kalsi *et al.* (2023)[13] observed a similar structure with 15 neurons as most effective for microwave drying of stevia leaves. Zalpouri *et al.* (2025)[30] reported effective MR predictions for refractance window drying of coriander puree with 10 hidden neurons. The results indicate that an ANN is effective at modelling thin-layer drying of SLP. In addition to predictive accuracy, ANN models can assist in process monitoring and optimization by capturing complex relationships between drying variables, which may support improved control of drying operations and potential scale-up.

3.4. Comparison of the best mathematical drying model with the ANN model

The best-performing mathematical drying model was compared with the ANN model in predicting moisture content in SLP during hot-air drying. The comparison between R^2 and χ^2 of Logarithmic and ANN models was tabulated in Table 4. The results indicated that the ANN model performance better than the logarithmic model, with slightly better predictive performance, as evidenced by a higher R^2 value and lower χ^2. This observation is consistent with previously reported studies, in which ANN models demonstrated improved prediction of drying behaviour compared with traditional empirical models. These findings are consistent with the previous studies, such as Zalpouri *et al.* (2025)[30] for coriander puree dried using a refractance window, Tarafdar *et al.* (2021)[31] for vacuum drying of moringa leaves, Tarafdar *et al.* (2025)[32] for freeze-drying of button mushrooms, and Zalpouri *et al.* (2023)[12] for onion puree dried by a refractance window. Therefore, the present results further support the applicability of ANN as a complementary modelling approach for describing the thin-layer drying behaviour of SLP.

3.5. Scanning electron microscopy. In Fig. 7, SEM images show the surface characteristics of SLP from both untreated and CP-treated samples (45 kV) for 5, 10, and 15 min. The control exhibited a smooth surface with minimal microstructural defects and served as a reference for comparison. The sample

Table 4 R^2 and χ^2 of Logarithmic and ANN model

	Logarithmic model		ANN model	
Sample	R^2	χ^2	R^2	χ^2
Control	0.99004	0.00983	0.99989	0.09960
CP/05 min	0.99472	0.00451	1.00000	0.00006
CP/10 min	0.99603	0.00314	0.99998	0.03358
CP/15 min	0.9972	0.0021	1.00000	0.00018

treated with CP for 5 min initiated surface etching, characterized by a rough surface, discrete pits, and enhanced porosity. The effect became more pronounced when the treatment was extended to 10 min, resulting in pronounced morphological modifications, including deeper etching, enlarged pores, and the onset of microcracks, which enhanced the surface available for drying and thus improved the drying rate. When the plasma treatment was extended to 15 min, the sample surface showed maximum etching, characterized by severe roughening, extensive pore formation, and visible surface damage, including fiber thinning and surface cracking.

These findings confirm that excessive plasma exposure resulted in adverse effects on SLP integrity, induced by reactive species generated during the plasma discharge, leading to oxidation, bond cleavage, and micro-etching. The phenomenon can enhance surface hydrophilicity by generating new functional groups, facilitating moisture removal during drying, and enabling the extraction of more bioactives than the control sample. CP treatment induced progressive surface modification and increased porosity with increasing exposure time, consistent with reports on CP-treated Bambara, chilli, and papaya seeds and on millet-based analogue rice, which showed a rougher, more porous surface than the control.[33,34]

The formation of plasma-induced microchannels altered the mass transfer pathway, directly contributing to increased moisture diffusivity and improved rehydration behavior, and demonstrating a clear structure-process quality relationship. Nevertheless, quantitative image analyses such as pore size distribution and surface roughness evaluation were not carried out in the present work and may provide deeper understanding of the microstructural alterations caused by plasma treatment.

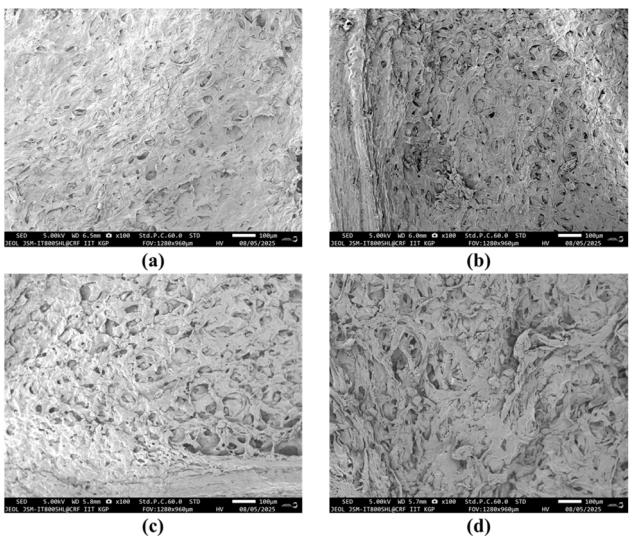

Fig. 7 Microstructural changes in SLP: control and under different (a) cold plasma pre-treatment, CP/05 min (b), CP/10 min (c), and CP/15 min (d).

3.6. Rehydration ratio

RR is a critical parameter for dried products, as the products are generally rehydrated before consumption. In the present study, the RR of SLP was impacted by CP pre-treatment duration (Table 5). The control sample showed an RR of 2.96, whereas the CP-treated sample showed improvement in RR, with values of 3.14 (5 min), 3.26 (10 min), and 3.37 (15 min). The results indicated that CP pre-treatment enhances SLP's RR ability, with 15 minutes of exposure resulting in the most pronounced effect. The increase in RR could be attributed to etching of the peel surface, leading to the formation of micropores. The formed micropores increase surface area, enabling faster, more efficient absorption during rehydration. In addition, the generated ROS resulted in surface-level modifications that improve surface hydrophilicity and affinity towards water molecules.[24,25] These effects become more pronounced with increasing CP exposure duration.

A similar improvement in RR due to CP pre-treatment has been reported in previous studies. Subrahmanyam *et al.* (2024) reported that 10 min CP pre-treatment resulted in a 21.63% increase in the RR of dried apple slices. Similarly, Zhou *et al.* (2020)[19] observed that a short exposure of CP (15–60 s) enhanced the RR of dried wolfberry by 7–16%.

3.7. Total phenolic content

TPC content of the control sample (18.74 mg GAE/g db) was significantly ($p < 0.05$) lower than the CP-pretreated samples (Table 5). The TPC value increased with treatment time up to 10 min, where the maximum value was observed, nearly 41% higher than the control. This enhancement is likely associated with plasma-induced disruption of cell walls and the release of bound phenolics caused by reactive species generated during CP treatment, which may also enhance diffusion of phenolic compounds during treatment.[6,35] Similar findings were reported by Subrahmanyam *et al.* (2024)[36] in hot-air-dried apple slices, Zhou *et al.* (2020)[19] in wolfberry, and Karim *et al.* (2021)[37] in shiitake mushrooms, attributing the significant increase in phenols at the end of the drying process. However, further exposure to CP (15 min) resulted in a decline to 22.42 mg GAE/g, although the value remained significantly higher than the control.

3.8. Total flavonoid content

Flavonoid content followed a similar trend, with the control sample having the lowest TFC (15.23 mg QE/g). CP treatment significantly increased flavonoid levels, reaching a maximum of 26.73 mg QE/g at 10 minutes, approximately 75% higher than the control. This increase may similarly be attributed to plasma-induced cellular disruption, which facilitates the release and

Table 5 Effect of Cold Plasma Treatment on quality parameters of SLP

Sample	Rehydration ratio	TPC (mg GAE per g db)	TFC (mg QE per g db)	Antioxidant activity (%)	Ascorbic acid (mg/100g)
Control	2.96 ± 0.09^{c}	18.74 ± 0.63^{d}	15.23 ± 0.46^{d}	32.38 ± 1.19^{c}	60.12 ± 0.3^{d}
CP/5 min	3.14 ± 0.01^{b}	20.65 ± 0.22^{c}	20.74 ± 0.02^{c}	35.93 ± 0.09^{b}	68.33 ± 0.91^{c}
CP/10 min	3.26 ± 0.03 ^{ab}	26.53 ± 0.14^{a}	26.73 ± 0.46^{a}	44.88 ± 1.38^{a}	82.28 ± 0.34^{a}
CP/15 min	3.37 ± 0.09^{a}	22.42 ± 0.14^{b}	22.68 ± 0.15^{b}	38.18 ± 1.37^{b}	71.14 ± 0.58^{b}

Values were expressed as Mean ± standard deviation of three replications. Mean values in the same column with different superscripts (a–d) are significantly different ($p \leq 0.05$).

diffusion of flavonoids during treatment.[6,35] However, prolonged CP treatment (*i.e.*, 15 min) resulted in a decline in TFC, which remained higher than in the control sample. Seelarat *et al.* (2024)[38] reported a 25.77% enhancement of TFC in dried jackfruit slices when pre-treated with dielectric barrier discharge plasma. The findings were also supported by the studies on dried apple slices,[36] dried jujube,[24] and dried shiitake mushrooms.[39]

3.9. DPPH radical scavenging activity

Antioxidant Activity (AA) showed a similar time-dependent trend to phenols and flavonoids. The control sample showed the lowest value of 32.38%. The AA significantly improved to 35.93% after 5 minutes and increased to 44.88% after 10 minutes of CP treatment. This improvement is likely associated with increased levels of phenolics, flavonoids, and vitamin C, which collectively contribute to antioxidant potential and enhance radical-scavenging activity.[40] Prolonged exposure reduced AA by 38.18% at 15 minutes, suggesting the onset of oxidative degradation under extended plasma exposure. These results are in accordance with the previous findings from CP-treated apple slices,[36] raisins[41] and jackfruit slices.[38]

3.10. Ascorbic acid

Ascorbic acid was lowest in the control sample (60.12 mg/100 g), while CP pretreatment significantly enhanced retention ($p < 0.05$). The highest ascorbic acid retention was recorded at 10 min, 37% higher than the control. The improved retention may be related to plasma-induced surface modifications that help protect ascorbic acid from thermal and oxidative degradation during drying. Additionally, plasma-generated reactive nitrogen species, such as nitric oxide, may activate dehydroascorbate reductase, promoting ascorbic acid regeneration and further improving its stability.[42,43] However, longer CP exposure (>10 min) resulted in a decline in ascorbic acid (71.14 mg/100 g), which may be associated with increased oxidative damage caused by reactive oxygen species generated during plasma treatment.[44] Ashtiani *et al.* (2020)[41] reported that CP pre-treatment resulted in 40.90% and 17.94% ascorbic acid retention in dried grapes treated for 50 s and 10 s, respectively. Furthermore, Subrahmanyam *et al.* (2024)[36] reported that CP enhances ascorbic acid concentration, but prolonged exposure results in its decline.

The results of this study showed that bioactive compounds increased up to 10 min of CP exposure but declined at 15 min.

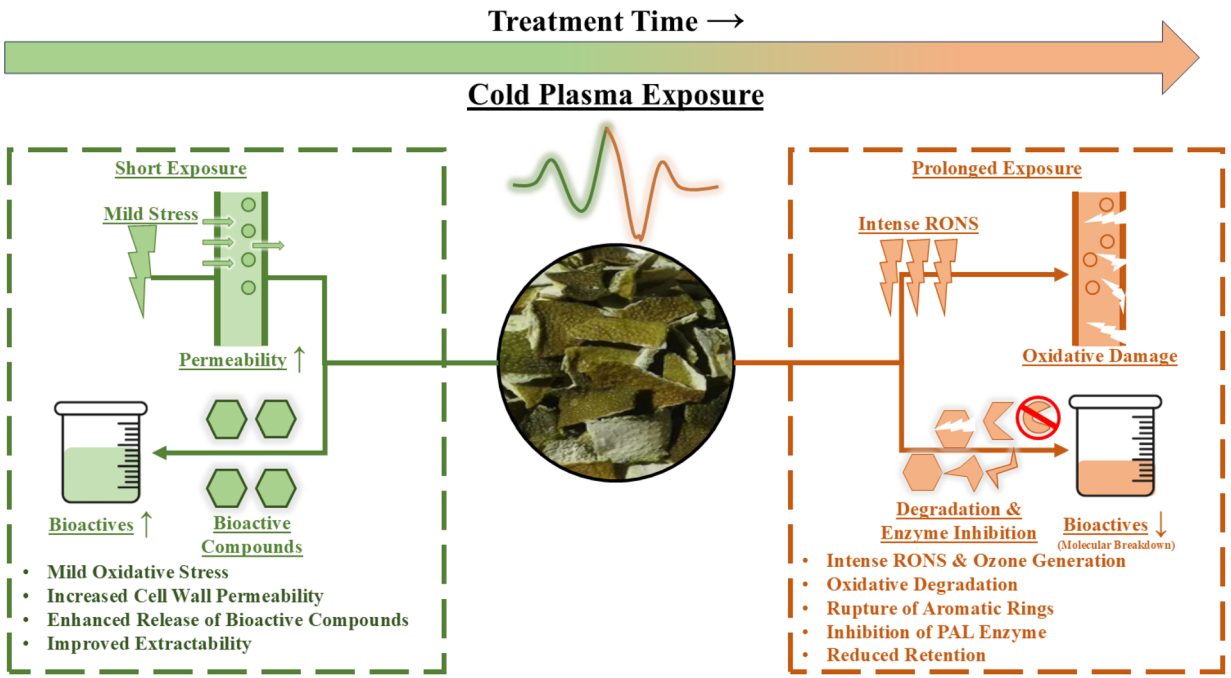

Fig. 8 Impact of cold plasma on bioactives components.

This reduction may be attributed to oxidative mechanisms induced by plasma-generated reactive species. During plasma discharge, previous studies report that high-energy electrons can dissociate molecular oxygen into atomic oxygen, which may subsequently react with other oxygen molecules to form ozone. Molecular ozone is considered a strong oxidizing agent capable of degrading bioactive compounds by disrupting their aromatic ring structures.[45] Moreover, prolonged exposure to reactive oxygen and nitrogen species has been reported to inhibit or denature phenylalanine ammonia-lyase (an enzyme involved in the biosynthesis of phenolic compounds), thereby limiting further phenolic accumulation.[46]

In contrast, shorter plasma exposure may induce mild oxidative stress, improving cell permeability and promoting the release of bound bioactives without significant molecular degradation.[6,35] This dual behavior explains the increase in bioactives at moderate treatment times, followed by a decline at extended exposure.

In short, the response of bioactive compounds to CP exposure showed a non-linear, time-dependent pattern, indicating that moderate treatment enhances bioactive release, whereas excessive exposure becomes detrimental (Fig. 8).

4 Conclusion

CP pre-treatment was demonstrated to be an effective non-thermal technology for enhancing drying efficiency and improving quality retention of SLP, a major citrus by-product. Among all the pre-treatment conditions tested, a 10 minute exposure was identified as the optimal treatment time, providing the balance between accelerated drying and retention of bioactive components, including phenolics, flavonoids, vitamin C, and antioxidant activity. Structural analysis indicated that plasma-induced microchannel formation, enhanced moisture diffusion during hot-air drying.

CP pretreatment at 45 kV for 10 min enhanced moisture removal from SLP, reducing oven drying time from 150 min to 112.13 min and lowering thermal energy consumption by approximately 25%. The improved drying efficiency and preservation of nutritional quality highlight CP-assisted drying as a sustainable approach for converting citrus processing waste into value-added products. In this reference, the approach supports SDG 2 (Zero Hunger) by promoting the use of nutrient-rich by-products in the food chain, SDG 9 (Industry, Innovation, and Infrastructure) by adoption of innovative, energy-efficient non-thermal processing techniques, and SDG 12 (Responsible Consumption and Production) by advancing waste reduction and circular economy practices within the food processing industries.

The study showed that the ANN model predicted moisture ratio with slightly higher accuracy than traditional mathematical drying models, consistent with previous studies and supporting its potential use as a complementary tool for modeling and optimizing the drying process. Although prolonged CP exposure (15 minutes) led to a decline in bioactive retention, the levels remained higher than those of untreated samples, underscoring the importance of optimizing pre-treatment conditions.

The study provides an application-oriented evaluation and optimization of CP pre-treatment for SLP drying. The findings demonstrate practical feasibility at laboratory scale; however, further pilot- and industrial-scale investigations are necessary to assess scalability, economic viability, and long-term operational performance before large-scale implementation.

Author contributions

Gurveer Kaur: methodology, data curation, conceptualization, writing – original draft, writing – review & editing. Sandhya Singh: investigation, writing – review & editing, supervision, resources, project administration. Vimal Challana: investigation, writing – original draft, writing – review & editing, formal analysis, data curation, conceptualization. Sumandeep Kaur: formal analysis, data curation, investigation, software.

Conflicts of interest

There are no conflicts to declare.

Abbreviations

ANN	Artificial neural network
CP	Cold plasma
DBD	Dielectric barrier discharge
DPPH	1,1-Diphenyl-2-picryl hydrazyl
DR	Drying rate
MSE	Mean squared error
MR	Moisture ratio
R^2	Coefficient of determination
RMSE	Root mean square error
ROS	Reactive oxygen species
RR	Rehydration ratio
SLP	Sweet Lime Peel
TFC	Total flavonoid content
TPC	Total phenolic content
χ^2	Chi-square

Data availability

Data analyzed and recorded during the research are included in this article.

Acknowledgements

The authors gratefully acknowledge the Department of Science and Technology, Government of India and Punjab Agricultural University, Ludhiana, for the facilities and support extended during the course of this study.

References

1 S. Suri, A. Singh, P. K. Nema, S. Malakar and V. K. Arora, *Food Biosci.*, 2022, **48**, 101789.
2 A. Sánchez-Elvira, E. Hernández-Corroto, M. C. García, M. Castro-Puyana and M. L. Marina, *Food Chem.*, 2024, **458**, 140139.

3 C. Bessa, T. Francisco, R. Dias, N. Mateus, V. d. Freitas and R. Pérez-Gregorio, *Front. Sustain. Food Syst.*, 2021, **5**, 623611.
4 D. I. Onwude, N. Hashim, K. Abdan, R. Janius, G. Chen and C. Kumar, *J. Food Eng.*, 2018, **228**, 12–24.
5 L. A. Yanclo, Z. A. Belay, G. O. Sigge and O. J. Caleb, *Heliyon*, 2023, **9**, e18555.
6 G. Kaur, Sandhya, M. Kaur, V. Challana and S. Kaur, *Qual. Assur. Saf. Crops Foods*, 2025, **17**, 163–189.
7 S. S. Shirkole, R. Jayabalan and P. P. Sutar, *Innovative Food Sci. Emerging Technol.*, 2020, **62**, 102345.
8 B. S. Kalsi, S. Singh, M. S. Alam and G. K. Sidhu, *Int. J. Food Prop.*, 2023, **26**, 3356–3375.
9 L. Zhu, M. Li, W. Yang, J. Zhang, X. Yang, Q. Zhang and H. Wang, *Foods*, 2023, **12**, 1652.
10 N. Mahmood, Y. Liu, Z. Munir, Y. Zhang and B. M. K. Niazi, *LWT*, 2022, **158**, 113131.
11 S. S. Shirkole and P. P. Sutar, *Drying Technol.*, 2019, **37**, 253–267.
12 R. Zalpouri, M. Singh, P. Kaur, A. Kaur, K. K. Gaikwad and A. Singh, *Processes*, 2023, **11**, 700.
13 B. S. Kalsi, S. Singh, M. S. Alam and S. Bhatia, *J. Food Qual.*, 2023, **2023**, 2811491.
14 Y. F. Paiva, R. M. F. d. Figueirêdo, A. J. d. M. Queiroz, J. P. d. L. Ferreira, F. S. d. Santos, C. G. d. Reis, L. T. S. Amadeu, A. G. B. d. Lima, J. P. Gomes, W. P. d. Silva, P. B. Maracajá and C. C. Costa, *Processes*, 2023, **11**, 888.
15 G. M. White, I. J. Ross and C. G. Poneleit, *Trans. ASAE*, 1981, **24**, 466–0468.
16 E. P. d. Sousa, E. N. A. d. Oliveira, T. L. S. Lima, R. F. Almeida, J. H. T. Barros, C. M. G. Lima, A. M. Giuffrè, J. Wawrzyniak, S. Wybraniec, H. D. M. Coutinho and B. F. Feitosa, *Foods*, 2024, **13**, 2784.
17 S. Ambawat, A. Sharma and R. K. Saini, *Processes*, 2022, **10**, 2464.
18 J.-W. Bai, D.-D. Li, R. Abulaiti, M. Wang, X. Wu, Z. Feng, Y. Zhu and J. Cai, *Foods*, 2025, **14**, 84.
19 Y.-H. Zhou, S. K. Vidyarthi, C.-S. Zhong, Z.-A. Zheng, Y. An, J. Wang, Q. Wei and H.-W. Xiao, *LWT*, 2020, **134**, 110173.
20 N. Phuyal, P. K. Jha, P. P. Raturi and S. Rajbhandary, *Sci. World J.*, 2020, **2020**, 8780704.
21 S. Baliyan, R. Mukherjee, A. Priyadarshini, A. Vibhuti, A. Gupta, R. P. Pandey and C. M. Chang, *Molecules*, 2022, 27.
22 S. S. Nielsen, in *Nielsen's Food Analysis Laboratory Manual*, ed. B. P. Ismail and S. S. Nielsen, Springer International Publishing, Cham, 2024, pp. 153–156, DOI: 10.1007/978-3-031-44970-3_18.
23 A. d. C. Loureiro, F. d. C. d. A. Souza, E. A. Sanches, J. d. A. Bezerra, C. V. Lamarão, S. Rodrigues, F. A. N. Fernandes and P. H. Campelo, *Food Res. Int.*, 2021, **147**, 110462.
24 T. Bao, X. Hao, M. R. I. Shishir, N. Karim and W. Chen, *J. Sci. Food Agric.*, 2022, **102**, 1030–1039.
25 V. Rathore, B. S. Tiwari and S. K. Nema, *Plasma Chem. Plasma Process.*, 2022, **42**, 109–129.
26 X.-L. Zhang, C.-S. Zhong, A. S. Mujumdar, X.-H. Yang, L.-Z. Deng, J. Wang and H.-W. Xiao, *J. Food Eng.*, 2019, **241**, 51–57.
27 Q. Chen, J. Bi, X. Wu, J. Yi, L. Zhou and Y. Zhou, *LWT–Food Sci. Technol.*, 2015, **64**, 759–766.
28 E. K. Akpinar and Y. Bicer, *Energy Convers. Manage.*, 2008, **49**, 1367–1375.
29 A. Y. Khaled, A. Kabutey, K. Ç. Selvi, Č. Mizera, P. Hrabe and D. Herák, *Processes*, 2020, **8**, 544.
30 R. Zalpouri, M. Singh, P. Kaur, S. Singh, S. Kumar and A. Kaur, *Biomass Convers. Biorefin.*, 2025, **15**, 967–983.
31 A. Tarafdar, N. Jothi and B. P. Kaur, *J. Appl. Res. Med. Aromat. Plants*, 2021, **24**, 100306.
32 A. Tarafdar, N. C. Shahi and A. Singh, *Neural Comput. Appl.*, 2019, **31**, 7257–7268.
33 S. G. Kishore, M. Dwivedi, R. Rahul, J. Deepa, G. Jeevarathinam, K. Kamaleeswari, G. Jothiprakash and A. Veluswamy, *Sustainable Food Technol.*, 2025, **4**(1), 1057–1072.
34 N. Ahmed, K. S. Siow, M. F. M. R. Wee and A. Patra, *Sci. Rep.*, 2023, **13**, 1675.
35 Y. Bao, L. Reddivari and J.-Y. Huang, *Innovative Food Sci. Emerging Technol.*, 2020, **65**, 102445.
36 K. Subrahmanyam, K. Gul, S. Paridala, R. Sehrawat, K. S. More, M. Dwivedi and S. Jaddu, *Innovative Food Sci. Emerging Technol.*, 2024, **92**, 103594.
37 N. Karim, M. R. I. Shishir, T. Bao and W. Chen, *J. Sci. Food Agric.*, 2021, **101**, 6271–6280.
38 W. Seelarat, S. Sangwanna, T. Chaiwon, T. Panklai, N. Chaosuan, A. Bootchanont, C. Wattanawikkam, P. Porjai, W. Khuangsatung and D. Boonyawan, *J. Sci. Food Agric.*, 2024, **104**, 3654–3664.
39 M. R. I. Shishir, N. Karim, T. Bao, V. Gowd, T. Ding, C. Sun and W. Chen, *Drying Technol.*, 2020, **38**, 2134–2150.
40 Y. M. Muflihah, G. Gollavelli and Y.-C. Ling, *Antioxidants*, 2021, **10**, 1530.
41 S.-H. Miraei Ashtiani, M. Rafiee, M. Mohebi Morad, M. Khojastehpour, M. R. Khani, A. Rohani, B. Shokri and A. Martynenko, *Innovative Food Sci. Emerging Technol.*, 2020, **63**, 102381.
42 C. Shan, Y. Zhou and M. Liu, *Protoplasma*, 2015, **252**, 1397–1405.
43 C. Sun, L. Liu, Y. Yu, W. Liu, L. Lu, C. Jin and X. Lin, *J. Integr. Plant Biol.*, 2015, **57**, 550–561.
44 Y. Li, X. Huang, Y. Yang, A. Mulati, J. Hong and J. Wang, *Foods*, 2025, **14**, 149.
45 F. D. L. Almeida, R. S. Cavalcante, P. J. Cullen, J. M. Frias, P. Bourke, F. A. N. Fernandes and S. Rodrigues, *Innovative Food Sci. Emerging Technol.*, 2015, **32**, 127–135.
46 C. Sarangapani, G. O'Toole, P. J. Cullen and P. Bourke, *Innovative Food Sci. Emerging Technol.*, 2017, **44**, 235–241.